



Solar-driven photocatalytic degradation of phenol in aqueous solution using visible light active carbon-modified (CM)-n-TiO₂ nanoparticles

Yasser A. Shaban^{a,b}

^aFaculty of Marine Sciences, Marine Chemistry Department, King Abdulaziz University, P.O. Box 80207, Jeddah 21589, Saudi Arabia

^bNational Institute of Oceanography & Fisheries, Qayet Bay, Alexandria, Egypt
Tel. +966 595670522; Fax: +966 26401747; email: yasrsh@yahoo.com

Received 17 March 2013; Accepted 2 September 2013

ABSTRACT

Visible light active carbon-modified (CM)-n-TiO₂ nanoparticles were synthesized by sol/gel method. Carbon modification of n-TiO₂ was performed during the synthesis process by using titanium butoxide as a carbon source in addition of being a molecular precursor of TiO₂. When compared to unmodified n-TiO₂, CM-n-TiO₂ nanoparticles exhibited significantly higher photocatalytic activity toward the photocatalytic degradation of phenol in aqueous solution under illumination of both UV light and real sunlight. Carbon modification was found to be responsible for narrowing the bandgap energy of CM-n-TiO₂ from 3.14 to 1.86 eV. The effects of catalyst dose, initial concentration of phenol, and pH on the degradation kinetics of phenol were investigated. The highest degradation rate of phenol was obtained at the optimal conditions of pH 5 and 1.0 g L⁻¹ of CM-n-TiO₂. The photocatalytic degradation of phenol using CM-n-TiO₂ obeyed a pseudo-first-order kinetics according to the Langmuir–Hinshelwood model.

Keywords: Photocatalytic degradation; Phenol; Titanium oxide; Carbon modification

1. Introduction

The contamination of water supplies with hazardous phenolic compounds is a serious problem in terms of environmental considerations, due to their toxicity, high stability, and bioaccumulation nature [1]. Conventional treatment processes to remove these pollutants, such as chlorination [2,3], solvent extraction [4,5], adsorption [6], and membrane process [7–9] have several limitations and drawbacks. These processes are either costly or have the inherent drawbacks due to the tendency of the formation of secondary toxic materials [10,11]. Therefore, the

development of an effective and inexpensive water purification process to remove these compounds without leaving behind any hazardous residues has become a challenge.

In recent years, solar photochemical detoxification of polluted waters using nanostructured titanium dioxide (TiO₂) has been proposed as an effective and economical method to convert organic pollutants in contaminated water and air to carbon dioxide, water and mineral acids, which are less toxic substances [12]. Titanium dioxide was recognized to be the most promising semiconductor; it has been widely used as a catalyst because of its merits, including optical and

electronic properties, low cost, high level of photocatalytic activity, chemical stability, and nontoxicity. Over the past several years, heterogeneous semiconductor photocatalysis using titanium dioxide has received considerable attention for its application in water splitting to produce hydrogen [13–22], degradation of organic pollutants [23–26], and wastewater treatment [27,28]. However, one of the main shortcomings is the fact that titanium dioxide ($n\text{-TiO}_2$) is a UV absorber. Its wide band gap (3.0–3.2 eV) limits its photoresponse in the ultraviolet region which is only a small fraction (~5%). Therefore, several attempts were made to extend its optical response to the visible spectral range by doping with transition metal [29,30], nitrogen [31,32], and sulfur [33]. Recently, it was found that carbon modification of $n\text{-TiO}_2$ photocatalyst lowered its bandgap energy to 2.32 eV [16]. This progress stimulated further investigations on carbon-modified $n\text{-TiO}_2$ as visible light active photocatalyst [17–22,26].

However, most of the studies on heterogeneous photocatalytic decomposition of phenolic compounds using $n\text{-TiO}_2$ have been focused on the utilization of UV as a light source. Therefore, in the present study, visible light active carbon-modified (CM)- $n\text{-TiO}_2$ nanoparticles that are capable of harvesting the maximum light photons in the visible and UV regions of solar light were prepared from carbon-containing precursor, titanium butoxide, no external source of carbon was used. The photocatalytic performance of CM- $n\text{-TiO}_2$ was examined for the degradation of phenol in aqueous solution under illumination of natural sunlight in addition to UV light. The photocatalytic activity of CM- $n\text{-TiO}_2$ was compared with regular $n\text{-TiO}_2$. The effects of various experimental parameters such as photocatalyst loading, phenol concentration, and pH on the photocatalytic removal rate of phenol were studied. Furthermore, photodegradation kinetics of phenol was studied and discussed in terms of Langmuir–Hinshelwood model.

2. Materials and methods

2.1. Chemicals and reagents

All chemicals were of analytical grade and were used without any further purification: titanium butoxide (Fluka, 97%); titanium trichloride (Sigma–Aldrich, TiCl_3 12% in hydrochloric acid (5–12%)); phenol (Aldrich, 99 + %); and ethanol (Sigma–Aldrich, HPLC). Hydrochloric acid and NaOH (analytical grade) were used for pH adjustment. Solutions were prepared with ultra-pure water obtained using a Millipore device (Milli-Q).

2.2. Photocatalysts preparation and characterization

Visible light active carbon-modified titanium dioxide (CM- $n\text{-TiO}_2$) nanoparticles were synthesized by a sol/gel method. About 30 mmol of titanium butoxide was dissolved in 10 mL anhydrous ethanol. Five milliliters of water was added dropwise under vigorous stirring. The pH was adjusted between 3 and 4. The resulting gel was then stirred for 2 h at room temperature, aged for 24 h at ambient temperature, and finally dried at 100 °C for 12 h to form a precursor. CM- $n\text{-TiO}_2$ nanoparticles were obtained by calcination of the precursor at 500 °C for 2 h. Regular (unmodified) titanium dioxide ($n\text{-TiO}_2$) nanoparticles were synthesized by hydrolysis and oxidation of titanium trichloride in an aqueous medium. Titanium trichloride was added dropwise under vigorous stirring into deionized water. The concentration of titanium was adjusted to 0.15 M. The pH of the obtained violet solution was adjusted between 3 and 4 with sodium hydroxide (NaOH) solution. The resulting solution was then heated at 80 °C in an oven for 24 h, followed by filtering, washing several times with distilled water, and then calcined at 300 °C for 2 h.

The Brunauer–Emmett–Teller surface area (S_{BET}) measurements of CM- $n\text{-TiO}_2$ and $n\text{-TiO}_2$ were carried out by N_2 adsorption at 77 K using a Quantachrome instrument. Samples were degassed at 100 °C for 1 h prior to S_{BET} measurements. The elemental composition of CM- $n\text{-TiO}_2$ and $n\text{-TiO}_2$ samples was performed using energy dispersive analyzer unit (EDAX Genesis) attached to the field emission scanning electron microscope (QUANT FEG 450, Amsterdam, The Netherlands). UV–vis light diffuse reflection spectra of CM- $n\text{-TiO}_2$ and $n\text{-TiO}_2$ were recorded using a Shimadzu UV–vis spectrophotometer (Model PharmaSpec UV-1700).

2.3. Photocatalytic degradation experiments

All photocatalytic experiments were carried out in a magnetically stirred 500-mL glass reactor loaded with the aqueous solution containing different concentrations of phenol ranging from 0.2 to 2 mg L^{-1} . The synthesized photocatalyst ($n\text{-TiO}_2$ or CM- $n\text{-TiO}_2$) was added with continuous stirring for uniform mixing.

For the experiments under UV light, the whole setup was placed inside Fluorescence Analysis Cabinet (Spetroline, Model: CC-80) equipped with a low-pressure UV fluorescent tube (8 W) emitting UV light of wavelength 254 nm. All solar photocatalytic experiments were carried out at the Faculty of Marine Sciences, Obhur, Jeddah, KSA, during July and August, 2011. The experiments were performed in the

daytime between 11:00 am and 15:00 pm. The photocatalytic reactor was directly exposed to natural sunlight. The average solar intensity was $1,200 \text{ W m}^{-2}$, measured by Field Scout Light Sensor Reader (Spectrum Technologies, Inc.) equipped with 3670i Silicon Pyranometer Sensor.

Aliquots of treated samples were regularly withdrawn from the reactor and centrifuged immediately to remove the catalyst. The phenol contents before and after photodegradation were analyzed according to Naley [34] using a spectrofluorometer (Shimadzu, Model: RF-5301 PC).

3. Results and discussion

3.1. Characterization of the photocatalysts

Table 1 shows the EDS results of regular n-TiO₂ and carbon-modified CM-n-TiO₂ nanoparticles. The presence of carbon (3.06 atomic% C) in CM-n-TiO₂ and its absence in n-TiO₂ were observed. The corresponding EDS spectra of n-TiO₂ and CM-n-TiO₂ are shown in Fig. 1. Note that carbon peak was observed for CM-n-TiO₂ (Fig. 1(B)) but not for n-TiO₂ (Fig. 1(A)).

From the S_{BET} measurements, the surface area of n-TiO₂ and CM-n-TiO₂ nanoparticles were found to be 53 and 34 $\text{m}^2 \text{ g}^{-1}$, respectively. These comparable values reveal that the S_{BET} will not be the dominant factor in comparing the photocatalytic performance of both catalysts.

The bandgap energies of n-TiO₂ and CM-n-TiO₂ were determined by establishing the Tauc plot [35] of the diffused reflectance spectra according to the following relations:

$$\alpha h\nu = A(h\nu - E_g)^n \quad (1)$$

where

$$\alpha = (1 - R)^2 \quad (2)$$

where h is Planck's constant, α is the absorption coefficient, ν is the frequency of vibration, E_g is the bandgap, A is the optical constant, n value is 1/2 for direct transitions and 2 for indirect transitions, and R is the

Table 1

Atomic percent of elements Ti, O, and C in n-TiO₂ and CM-n-TiO₂ from EDS data

Element	Atomic, %	
	n-TiO ₂	CM-n-TiO ₂
Ti	34.34	27.94
O	65.66	69.00
C	00.00	3.06

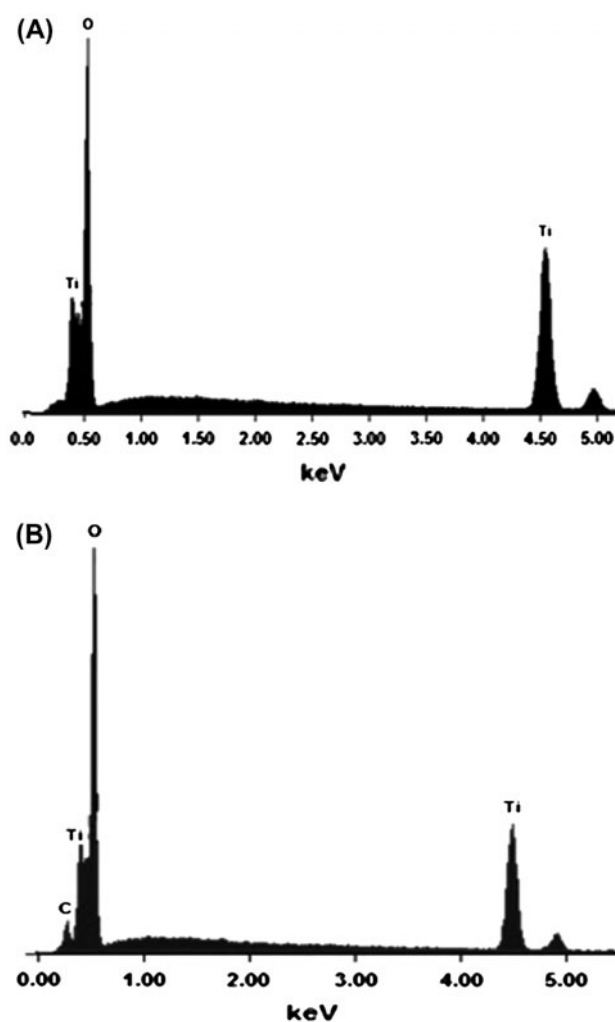


Fig. 1. Pattern of energy dispersive X-ray spectroscopy (EDS) for n-TiO₂ (A) and CM-n-TiO₂ (B).

diffused reflectance. The bandgap energy values determined from the Tauc plot (Fig. 2) were found to be 3.14 and 1.86 eV for n-TiO₂ and CM-n-TiO₂, respectively. The reduction of the bandgap of CM-n-TiO₂ can be attributed to the carbon incorporation during the synthesis of CM-n-TiO₂, and as a result, CM-n-TiO₂ nanoparticles may have higher visible light photocatalytic activity. The observed narrowing of the bandgap for CM-n-TiO₂ nanoparticles is in good agreement with the previously reported low bandgap values of 2.35 eV [16], 1.45 eV [22], and 1.6 eV [20] for carbon-doped TiO₂. Advanced theoretical studies also revealed that carbon doping is responsible for narrowing the bandgap energy of n-TiO₂ [36–38].

3.2. Photocatalytic activity of n-TiO₂ and CM-n-TiO₂

To evaluate the photocatalytic activity of CM-n-TiO₂, a comparison with unmodified n-TiO₂ under the same

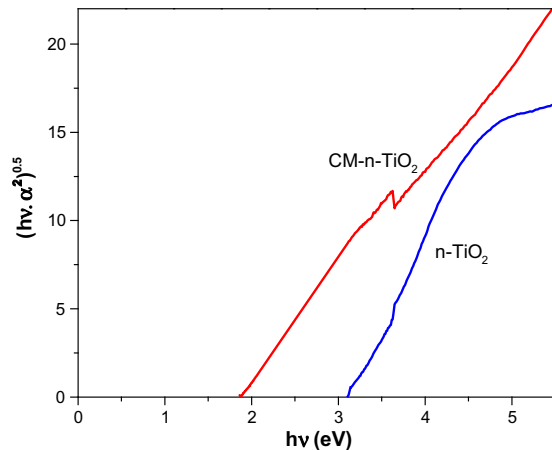


Fig. 2. Tauc plot for regular $n\text{-TiO}_2$ and CM-n-TiO_2 nanoparticles.

experimental conditions was performed. The degradation of phenol under artificial UV and natural sunlight illuminations was investigated. Fig. 3 illustrates the photodegradation of 1.0 mg L^{-1} of phenol under illumination of UV and real sunlight in the presence of 1.0 g L^{-1} of the photocatalyst. It is clearly observed that the photocatalytic activity of CM-n-TiO_2 is higher than that of $n\text{-TiO}_2$ under both UV and sunlight irradiation.

As can be seen in Fig. 3(a), the maximum percent of phenol removal using regular $n\text{-TiO}_2$ of 35% was observed after 240 min of UV irradiation, whereas in the presence of the same loading dose of CM-n-TiO_2 , only 150 min was needed to achieve complete degradation of phenol. Under sunlight illumination, complete disappearance of phenol (1.0 mg L^{-1}) was achieved after only 30 min when 1.0 g L^{-1} CM-n-TiO_2 was applied (Fig. 3(b)). After the same irradiation time, only 51.7% of phenol was degraded using regular $n\text{-TiO}_2$ under the same experimental conditions.

The enhanced photocatalytic activity of carbon-modified CM-n-TiO_2 nanoparticles can be attributed to carbon modification of TiO_2 , which helped in narrowing its bandgap [17–22].

3.3. Effect of catalyst dose on photodegradation

The influence of CM-n-TiO_2 dose on photodegradation of phenol (1.0 mg L^{-1}) under illumination of both UV light and natural sunlight was investigated. As shown in Fig. 4(a), the removal of phenol under UV irradiation is not apparently affected by the variations in the catalyst dose. This may be due to the limited number of UV light photons reaching the photocatalyst surface. Therefore, the increase in

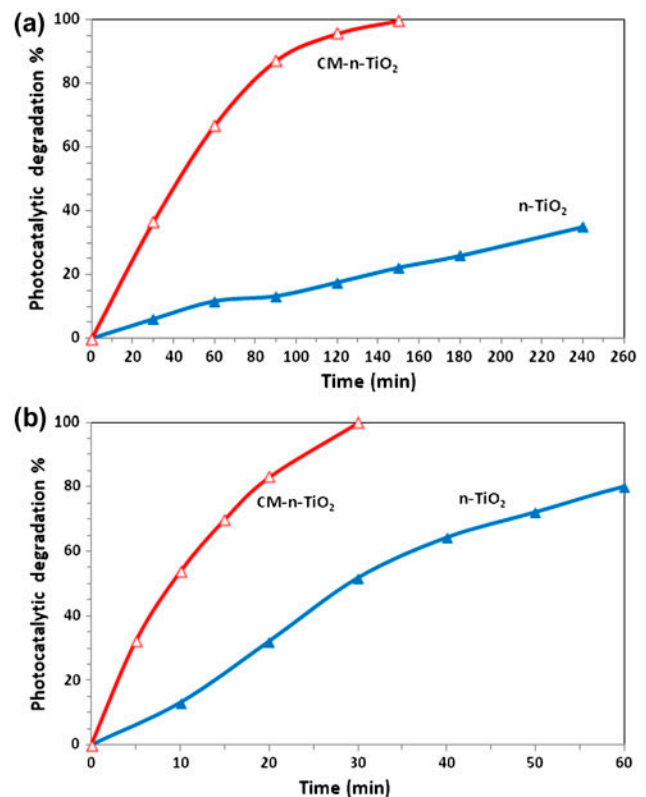


Fig. 3. Photocatalytic degradation of phenol (1.0 mg L^{-1}) in the presence of 1.0 g L^{-1} of CM-n-TiO_2 and $n\text{-TiO}_2$ under illumination of: (a) UV light; (b) natural sunlight.

catalyst loading may not significantly increase the active sites for photocatalytic reaction. On the other hand, the effect of CM-n-TiO_2 loading on photodegradation rate of phenol under illumination of natural sunlight is clearly observed (Fig. 4(b)). The solar photocatalytic degradation rate increased with the increase in catalyst dose from 0.5 to 1.0 g L^{-1} . Further increase in the catalyst loading to 1.5 g L^{-1} slightly decreased the degradation efficiency. This can be explained in terms of screening effects and light scattering. At catalyst loading beyond the optimum, the tendency toward particles aggregation increases, resulting in a reduction in surface area available for light absorption and hence a drop in photocatalytic degradation rate [39]. Additionally, the increase in the turbidity of the suspension reduces light penetration due to the enhancement of light scattering; the result is the decrease in the number of activated sites on the TiO_2 surface and shrinking of the effective photoactivated volume of suspension. The interplay of these two processes resulted in a reduced performance of photocatalytic activity with the overloaded catalyst [40,41]. Therefore, to ensure maximum absorption of efficient

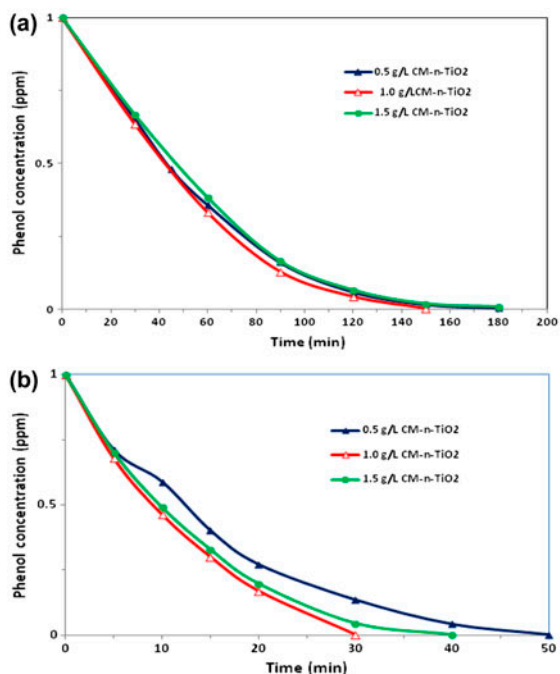
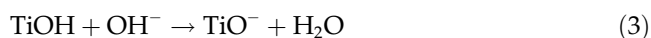


Fig. 4. Effect of CM-n-TiO₂ loading (0.5, 1.0, and 1.5 g L⁻¹) on photocatalytic degradation of 1.0 mg L⁻¹ of phenol under illumination of: (a) UV light; (b) natural sunlight.

photons and to avoid an ineffective excess amount of catalyst, the optimum catalyst loading must be determined. Hence, the optimal catalyst loading of 1.0 g L⁻¹ was employed throughout the present work.

3.4. Effect of solution pH on photodegradation

pH of the solution is an important parameter in the photocatalytic degradation of organic wastes as it is known to influence the surface charge of the semiconductor thereby affecting the interfacial electron transfer and the photoredox process [42]. The possible functional groups on TiO₂ surface in water are TiOH₂⁺, TiOH, and TiO⁻. The point of zero charge (pH_{pzc}) of TiO₂ is an important factor determining the distribution of the surface groups. When pH > pH_{pzc}, the surface of TiO₂ is negatively charged with the species TiO⁻ (Eq. (3)), and positively charged with the species TiOH₂⁺ at pH < pH_{pzc} (Eq. (4)).



The role of pH in the photocatalytic degradation of phenol under illumination of both UV and natural

sunlight using CM-n-TiO₂ was studied by keeping all other experimental conditions constant and varying the initial pH of the phenol solution from 3 to 9. As can be seen in Fig. 5, the degradation efficiency of CM-n-TiO₂ increases with the increase in pH from 3 to 5, beyond which the photodegradation efficiency starts to decrease, indicating an optimum pH of approximately 5 for best performance.

The pH of solution affects the formation of hydroxyl radicals as it can be inferred from the following equations [43]:



where e_{cb}^- represents a conduction band (CB) electron and h_{vb}^+ represents a positive hole in the valance band (VB) of the semiconductor.

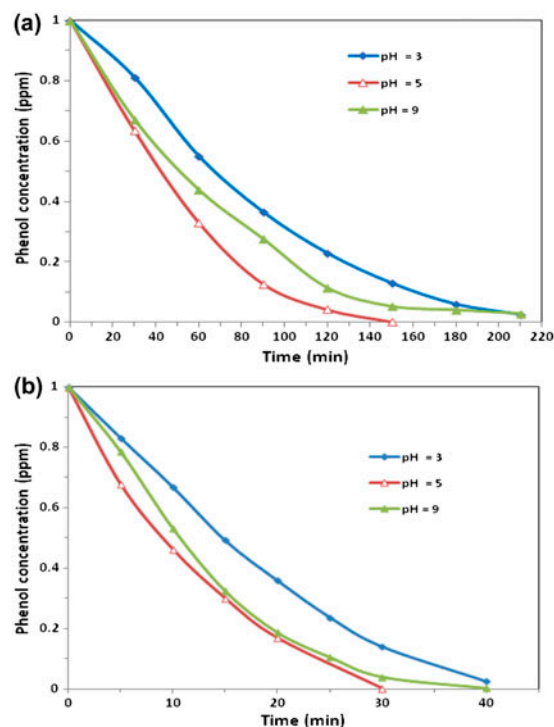
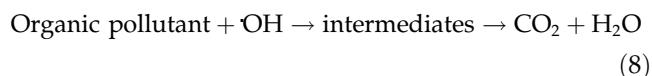


Fig. 5. Effect of pH on photocatalytic degradation of 1.0 mg L⁻¹ of phenol using 1.0 g L⁻¹ CM-n-TiO₂ under illumination of: (a) UV light; (b) natural sunlight.

As the high redox potentials of Eqs. (6) and (7) in acidic condition, the formation of hydroxyl radicals will be thermodynamically unfavorable [44]. As a result, the formation of hydroxyl radicals increased with an increase in pH from 3 to 5, resulting in an increased photocatalytic degradation efficiency of phenol. Besides, the undissociated state of the phenol species in pH 5 which favors its adsorption on the positively charged TiOH_2^+ surface. In an alkaline medium, the TiO_2 surface is negatively charged in a state of TiO^- and phenolate intermediate becomes dominant form [45], which may be repelled away from the TiO_2 surface which opposes the adsorption of substrate molecules on the surface of the catalyst. As a result, phenol degradation decreases in alkaline medium.

3.5. Effect of initial phenol concentration on photodegradation

The effect of the initial phenol concentration on its photodegradation rate was investigated over the range of 0.2 to 2.0 ppm using the optimum dose (1.0 g L^{-1}) of CM-n- TiO_2 as shown in Fig. 6.

It is clearly noted that the irradiation time required for complete removal of phenol under both UV (Fig. 6(a)) and natural sunlight (Fig. 6(b)) was extended as the initial phenol concentration increased. This can be explained in terms of the saturation of the limited number of accessible active sites on the photocatalyst surface and/or deactivation of the active sites of the catalyst. Several studies have reported that high organic substrate loadings induce the formation of intermediates that could be adsorbed onto the catalyst surface and deactivate the active sites [46,47]. Moreover, the significant absorption of light by the substrate at high concentrations might decrease the level of the light reaching the photocatalyst and thus its efficiency by reduction of the amount of OH^\cdot and O_2^- free radical production [48].

3.6. Photodegradation kinetics

The Langmuir–Hinshelwood (L–H) model is usually used to describe the kinetics of photocatalytic reactions of aquatic organics [49–52]. It basically relates the degradation rate (r) and reactant concentration in water at time t (C), which is expressed as follows:

$$r = -\frac{dc}{dt} = \frac{k_r K_{ad}}{1 + k_{ad} C} \quad (9)$$

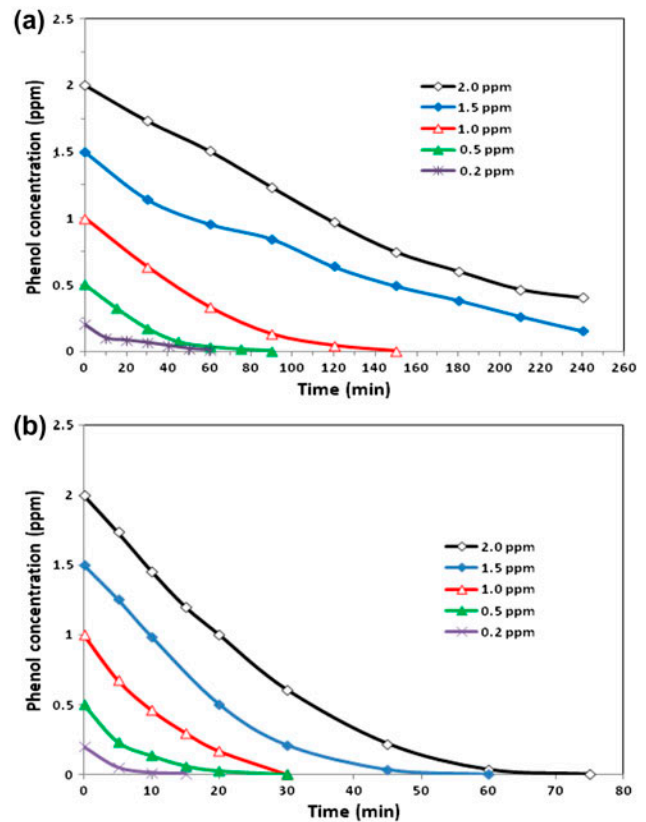


Fig. 6. Effect of initial concentration of phenol on its degradation using 1.0 g L^{-1} CM-n- TiO_2 under: (a) UV light; (b) natural sunlight.

where k_r is the rate constant and K_{ad} is the adsorption equilibrium constant. When the adsorption is relatively weak and/or the reactant concentration is low, Eq. (9) can be simplified to the pseudo-first-order kinetics with an apparent first-order rate constant k_{app} :

$$\ln\left(\frac{C_0}{C}\right) = K_r K_{ad} t = k_{app} t \quad (10)$$

where C_0 is the initial concentration. Plotting $\ln(C_0/C)$ vs. illumination time (t) yields a straight line, and the slope is the apparent rate constant k_{app} .

The photocatalytic degradation of phenol (1.0 mg L^{-1}) under both UV and natural sunlight illuminations at the optimal conditions of pH 5 and 1.0 g L^{-1} of CM-n- TiO_2 was successfully fitted using L–H model, and can be described by pseudo-first-order kinetic, as confirmed by the obtained straight line (Fig. 7(a)).

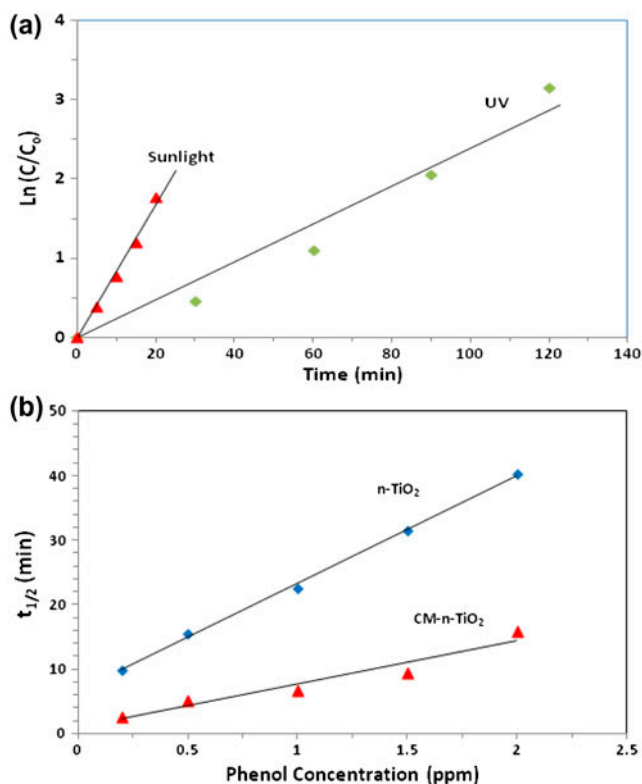


Fig. 7. Kinetic analysis of 1.0 mg L^{-1} phenol degradation under UV and natural sunlight (a) and half-life time reaction ($t_{1/2}$) values vs. initial phenol concentration in the presence of 1.0 g L^{-1} of CM-n-TiO₂ and n-TiO₂ under illumination of natural sunlight (b).

3.7. Half-life time reaction

The calculation of half-life time reaction ($t_{1/2}$) is one of the most useful means to evaluate the reaction rate of first order kinetic. At the half-life time of reaction, $C = 0.5 C_0$. For the reaction with the pseudo-first order, the half-life time can be calculated as the following:

$$t_{1/2} = \ln(2)/k_{\text{app}} \quad (11)$$

Table 2 lists the apparent first-order rate constant (k_{app}), and the calculated half-life time reaction ($t_{1/2}$) values for different phenol concentrations (0.2–2 ppm) under natural sunlight illumination at pH 5 using 1.0 g L^{-1} of CM-n-TiO₂ and n-TiO₂. It is interesting to note that the half-life time reaction ($t_{1/2}$) values for photocatalytic degradation of phenol using CM-n-TiO₂ are much smaller than those observed using regular n-TiO₂ (Fig. 7(b)). These results reveal that CM-n-TiO₂ nanoparticles have a better visible light harvesting ability than n-TiO₂, which can be attributed to the carbon modification that helped in lowering its bandgap energy.

Table 2

Apparent first-order rate constant (k_{app}) and the calculated half-life time reaction ($t_{1/2}$) values for different phenol concentrations

Phenol concentration (ppm)	k_{app} (min^{-1})		$t_{1/2}$ (min)	
	n-TiO ₂	CM-n-TiO ₂	n-TiO ₂	CM-n-TiO ₂
0.2	0.071	0.260	9.83	2.67
0.5	0.045	0.136	15.51	5.10
1.0	0.031	0.104	22.58	6.69
1.5	0.022	0.074	31.51	9.40
2.0	0.017	0.044	40.30	15.90

4. Conclusions

Visible light active carbon-modified (CM)-n-TiO₂ nanoparticles have been successfully synthesized via a sol/gel method. Carbon modification of n-TiO₂ was performed during the synthesis process by using titanium butoxide as molecular precursor of TiO₂ as well as a carbon source. CM-n-TiO₂ nanoparticles conferred significantly higher photocatalytic activity compared with unmodified n-TiO₂ toward the photocatalytic degradation of phenol in aqueous solution under illumination of both UV light and real sunlight. It is considered that carbon modification is responsible for lowering the bandgap energy of CM-n-TiO₂ nanoparticles, consequently significant enhancement in the photoactivity was observed. The efficiency of the photodegradation process has been observed to be strongly depended on catalyst dose, initial phenol concentration, and pH value. The experimental results indicated that the degradation rate of phenol was favorable at pH 5 and optimal catalyst dose of 1.0 g L^{-1} . The data of photocatalytic degradation of phenol using CM-n-TiO₂ were successfully fitted using Langmuir–Hinshelwood model and can be described by pseudo-first-order kinetic model.

Acknowledgments

This study was funded by the Deanship of Scientific Research (DSR), King Abdulaziz University, Jeddah, under the grant no. (330/150/431). The author, therefore, acknowledge with thanks DSR technical and financial support. The author is thankful to Mr Mousa Al Zobidi, Faculty of Marine Sciences, KAU, for his valuable help in the experimental analysis. The author would like to thank Dr Mohamed Mokhtar, Faculty of Sciences, KAU, for performing the S_{BET} measurements.

References

- [1] N.C. Saha, F. Bhunia, A. Kaviraj, Toxicity of phenol to fish and aquatic ecosystem, *Bull. Environ. Contam. Toxicol.* 63 (1999) 195–202.
- [2] F. Ge, L. Zhu, J. Wang, Distribution of chlorination products of phenols under various pHs in water disinfection, *Desalination* 225 (2008) 156–166.
- [3] V.K. Sharma, G.A.K. Anquandah, R.A. Yngard, H. Kim, J. Fekete, K. Bouzek, Nonylphenol, octylphenol, and bisphenol-A in the aquatic environment: A review on occurrence, fate, and treatment, *J. Environ. Sci. Health Part A* 44 (2009) 423–442.
- [4] V.M. Egorov, S.V. Smirnova, I.V. Pletnev, Highly efficient extraction of phenols and aromatic amines into novel ionic liquids incorporating quaternary ammonium cation, *Sep. Purif. Technol.* 63 (2008) 710–715.
- [5] R.S. Juang, T.P. Chung, M.L. Wang, D.J. Lee, Experimental observations on the effect of added dispersing agent on phenol biodegradation in a microporous membrane bioreactor, *J. Hazard. Mater.* 151 (2008) 746–752.
- [6] R.A. Shawabkeh, E.S.M. Abu-Nameh, Absorption of phenol and methylene blue by activated carbon from pecan shells, *Colloid J.* 69 (2007) 355–359.
- [7] M.S. Lee, C. Huang, K.R. Lee, J.R. Pan, W.K. Chang, Factors affecting phenol transfer through polydimethylsiloxane composite membrane, *Desalination* 234 (2008) 416–425.
- [8] H.R. Mortaheb, M.H. Amini, F. Sadeghian, B. Mokhtarani, H. Daneshyar, Study on a new surfactant for removal of phenol from wastewater by emulsion liquid membrane, *J. Hazard. Mater.* 160 (2008) 582–588.
- [9] H.S. Wu, C.C. Li, Kinetic study of phenol recovery using phase-transfer catalysis in horizontal membrane reactor, *Chem. Eng. J.* 144 (2008) 502–508.
- [10] G. Busca, S. Berardinelli, C. Resini, L. Arrighi, Technologies for the removal of phenol from fluid streams: A short review of recent developments, *J. Hazard. Mater.* 160 (2008) 265–288.
- [11] S. Patra, N. Munichandraiah, Electro-oxidation of phenol on polyethylenedioxythiophene conductive-polymer-deposited stainless steel substrate, *J. Electrochem. Soc.* 155 (2008) F23–F30.
- [12] M. Styliidi, P.L. Kondarides, X.E. Verykios, Visible light-induced photocatalytic degradation of Acid Orange in aqueous TiO₂ suspensions, *Appl. Catal. B* 47 (2004) 189–201.
- [13] A. Fujishima, K. Honda, Electrochemical photolysis of water at a semiconductor electrode, *Nature* 238 (1972) 37–38.
- [14] S.K. Mohapatra, M. Mishra, V.K. Mahajan, Design of a highly efficient photoelectrolytic cell for hydrogen generation by water splitting: Application of TiO_{2-x}C_x nanotubes as a photoanode and Pt/TiO₂ nanotubes as a cathode, *J. Phys. Chem. C* 111 (2007) 8677–8685.
- [15] S.U.M. Khan, J. Akikusa, Photoelectrochemical splitting of water at nanocrystalline n-Fe₂O₃ thin-film electrodes, *J. Phys. Chem. B* 103 (1999) 7184–7189.
- [16] S.U.M. Khan, M. Al-Shahry, W.B. Ingler, Jr. Efficient photochemical water splitting by a chemically modified n-TiO₂, *Science* 297 (2002) 2243–2245.
- [17] Y.A. Shaban, S.U.M. Khan, Efficient photoelectrochemical splitting of water to H₂ and O₂ at nanocrystalline carbon modified (CM)-n-TiO₂ and (CM)-n-Fe₂O₃ thin films, *Int. J. Nanotechnol.* 7 (2010) 69–98.
- [18] Y.A. Shaban, S.U.M. Khan, Efficient photoelectrochemical splitting of water to H₂ and O₂ at nanocrystalline carbon modified (CM)-n-TiO₂ thin films, *Solid State Phenomena* 162 (2010) 179–201.
- [19] Y.A. Shaban, S.U.M. Khan, Carbon modified (CM)-n-TiO₂ thin films for efficient water splitting to H₂ and O₂ under xenon lamp light and natural sunlight illuminations, *J. Solid State Electrochem.* 13 (2009) 1025–1036.
- [20] Y.A. Shaban, S.U.M. Khan, Visible light active carbon modified n-TiO₂ for efficient hydrogen production by photoelectrochemical splitting of water, *Int. J. Hydrogen Energy* 33 (2008) 1118–1126.
- [21] Y.A. Shaban, S.U.M. Khan, Surface grooved visible light active carbon modified (CM)-n-TiO₂ thin films for efficient photoelectrochemical splitting of water, *Chem. Phys.* 339 (2007) 73–85.
- [22] C. Xu, Y.A. Shaban, W.B. Ingler, Jr., S.U.M. Khan, Nanotube enhanced photoresponse of carbon modified (CM)-n-TiO₂ for efficient water splitting, *Sol. Energy Mater. Sol. Cells* 91 (2007) 938–943.
- [23] H. Park, W. Choi, Photocatalytic reactivities of nafion-coated TiO₂ for the degradation of charged organic compounds under UV or visible light, *J. Phys. Chem. B* 109 (2005) 11667–11674.
- [24] C. Burda, Y. Lou, X. Chen, A.C.S. Samia, J. Stout, J.L. Gole, Enhanced nitrogen doping in TiO₂ nanoparticles, *Nano Lett.* 3 (2003) 1049–1051.
- [25] K. Demeestere, J. Dewulf, B. De Witte, H. Van Langenhove, Visible light mediated photocatalytic degradation of gaseous trichloroethylene and dimethyl sulfide on modified titanium dioxide, *Appl. Catal. B* 61 (2005) 140–149.
- [26] C. Xu, R. Killmeyer, M.L. Gray, S.U.M. Khan, Photocatalytic effect of carbon-modified n-TiO₂ nanoparticles under visible light illumination, *Appl. Catal. B* 64 (2006) 312–317.
- [27] S. Parsons, *Advanced Oxidation Processes for Water and Wastewater Treatment*, IWA Publishing, Cornwall, 2004.
- [28] T. Oppenlander, *Photochemical Purification of Water and Air*, Wiley-VCH, Weinheim, 2003.
- [29] W. Choi, A. Termin, M.R. Hoffman, The role of metal ion dopants in quantum sized TiO₂: Correlation between photoreactivity and charge carrier recombination dynamics, *J. Phys. Chem.* 98 (1994) 13669–13679.
- [30] M. Anpo, Photocatalysis on titanium oxide catalysts: Approaches in achieving highly efficient reactions and realizing the use of visible light, *Catal. Surv. Jpn.* 1 (1997) 169–179.
- [31] R. Asahi, T. Morikawa, T. Ohwaki, K. Aoki, Y. Taga, Visible-light photocatalysis in nitrogen-doped titanium oxides, *Science* 293 (2001) 269–271.
- [32] Y.C. Hong, C.U. Bang, D.H. Shin, H.S. Uhm, Band gap narrowing of TiO₂ by nitrogen doping in atmospheric microwave plasma, *Chem. Phys. Lett.* 413 (2005) 454–457.
- [33] T. Umabayashi, T. Yamaki, H. Itoh, K. Asai, Band gap narrowing of titanium dioxide by sulfur doping, *Appl. Phys. Lett.* 81 (2002) 454–456.
- [34] A.M. Naley, Analysis of phenols in sea water by fluorometry: Direct analysis of the water phase, *Bull. Environ. Contam. Toxicol.* 31 (1983) 494–500.
- [35] T. Tauc, R. Grigorovici, A. Vancu, Optical properties and electronic structure of amorphous germanium, *Phys. Status Solidi B.* 15 (1966) 627–637.
- [36] X. Nie, K. Sohlberg, The influence of surface reconstruction and C-impurities on photocatalytic water dissociation by TiO₂, *MRC Proceedings*, 801 (2003) B205.
- [37] C.Di. Valentin, G. Pacchioni, A. Selloni, Theory of carbon doping of titanium dioxide, *Chem. Mater.* 17 (2005) 6656–6665.
- [38] H. Wang, J.P. Lewis, Effects of dopant states on photoactivity in carbon-doped TiO₂, *J. Phys.: Condens. Matter.* 17 (2005) L209–L211.
- [39] R. Wang, D. Ren, S. Xia, Y. Zhang, J. Zhao, Photocatalytic degradation of Bisphenol A (BPA) using immobilized TiO₂ and UV illumination in a horizontal circulating bed photocatalytic reactor (HCBPR), *J. Hazard. Mater.* 169 (2009) 926–932.
- [40] S. Merabet, A. Bouzaza, D. Wolbert, Photocatalytic degradation of indole in a circulating upflow reactor by UV/TiO₂ process—Influence of some operating parameters, *J. Hazard. Mater.* 166 (2009) 1244–1249.
- [41] M.L. Chin, A.R. Mohamed, S. Bhatia, Performance of photocatalytic reactors using immobilized TiO₂ film for the degradation of phenol and methylene blue dye present in water stream, *Chemosphere* 57 (2004) 547–554.

- [42] M.C. Lu, G.D. Roam, J.N. Chen, J.P. Huang, Factors affecting the photocatalytic degradation of dichlorovos over titanium dioxide supported on glass, *J. Photochem. Photobiol., A* 76 (1993) 103–109.
- [43] M. Nikazar, K. Gholivand, K. Mahanpoor, Photocatalytic degradation of azo dye Acid Red 114 in water with TiO₂ supported on clinoptilolite as a catalyst, *Desalination* 219 (2008) 293–300.
- [44] W.Z. Tang, C.P. Huang, Photocatalyzed oxidation pathways of 2,4-dichlorophenol by CdS in basic and acidic aqueous solutions, *Water Res.* 29 (1995) 745–756.
- [45] M. Bekbolet, I. Balcioglu, Photocatalytic degradation kinetics of humic acid in aqueous TiO₂ dispersions: The influence of hydrogen peroxide and bicarbonate ion, *Water Sci. Technol.* 34 (1996) 73–80.
- [46] R. Jain, M. Shrivastava, Photocatalytic removal of hazardous dye cyanosine from industrial waste using titanium dioxide, *J. Hazard. Mater.* 152 (2008) 216–220.
- [47] S. Ahmed, M.G. Rasul, W.N. Martens, R. Brown, M.A. Hashib, Heterogeneous photocatalytic degradation of phenols in wastewater: A review on current status and developments, *Desalination* 261 (2010) 3–18.
- [48] K.M. Parida, S.S. Dash, D.P. Das, Physico-chemical characterization and photocatalytic activity of zinc oxide prepared by various methods, *J. Colloid Interface Sci.* 298 (2006) 787–793.
- [49] A.V. Petukhov, Effect of molecular mobility on kinetics of an electrochemical Langmuir-Hinshelwood reaction, *Chem. Phys. Lett.* 277 (1997) 539–544.
- [50] K.H. Wang, Y.H. Hsieh, L.J. Chen, The heterogeneous photocatalytic degradation, intermediates and mineralization for the aqueous solution of cresols and nitrophenols, *J. Hazard. Mater.* 59 (1998) 251–260.
- [51] B. Bayarri, J. Gimenez, D. Curco, S. Esplugas, Photocatalytic degradation of 2,4-dichlorophenol by TiO₂/UV: Kinetics, actinometries and models, *Catal. Today* 101 (2005) 227–236.
- [52] E. Kusvuran, A. Samil, O.M. Atanur, O. Erbatur, Photocatalytic degradation kinetics of di- and tri-substituted phenolic compound in aqueous solution by TiO₂/UV, *Appl. Catal. B* 58 (2005) 211–216.